Hindawi
Advances in Materials Science and Engineering
Volume 2022, Article ID 1625327, 11 pages
https://doi.org/10.1155/2022/1625327

Research Article

Influence of Carbon Nanotubes on Enhancement of Sliding Wear Resistance of Plasma-Sprayed Yttria-Stabilised Zirconia Coatings

Chaithanya Kalangi and Venkateshwarlu Bolleddu

Department of Manufacturing, School of Mechanical Engineering, Vellore Institute of Technology, Vellore 632014, India

Correspondence should be addressed to Venkateshwarlu Bolleddu; venkateshwarlu.b@vit.ac.in

Received 29 August 2022; Revised 19 September 2022; Accepted 20 September 2022; Published 8 October 2022

Academic Editor: Temel Varol

An experimental investigation was performed to study the performance of thermally sprayed yttria stabilised zirconia (YSZ) coatings obtained with the reinforcement of carbon nanotubes (CNTs) in different weight percentage proportions. The atmospheric plasma spray (APS) method was used to deposit YSZ + CNTs at three different weight proportions on low carbon steel (AISI 1020) following the industrial standard procedure. The quality of thermally sprayed coatings was evaluated to report on percentage porosity (ASTM B276), sliding wear resistance (ASTM G133-05), and metallurgical bonding of the coating with the substrate material. From this investigation results, it has been confirmed that the thickness of the coatings is almost uniform, and the percentage porosity is decreased with an increase in CNTs weight percentage proportion. ImageJ software has confirmed the presence of CNTs in the ceramic deposit, and also uniform distribution throughout the coating. Subsequently, the metallurgical bonding of the deposit is also ensured and confirmed that the deposit adheres on the substrate. The hardness of the coating found increased with the increase in CNTs proportion as 554 Hv with 1 wt.% CNTs, 805 Hv with 3 wt.% CNTs, and 933 Hv with 5 wt.% CNTs in thermally sprayed YSZ. The results obtained are highly appreciable when compared to the hardness (454 Hv) of thermally sprayed pure YSZ coating. From results of wear tests, it was found that at slow speed (i.e., 319 rpm), the minimum mass loss was identified for all the three different combinations of CNTs reinforced coatings. However, 5 wt.% of CNTs in YSZ has very minimum wear at 5 kgf load and subsequently mass loss increased with the decrease in CNTs weight percentage proportion. Based on wear resistance, it was found that the 5 wt.% CNTs in YSZ has a maximum wear resistance. Severe wear scars and coating delamination in 1% CNTs reinforced coatings were identified from the microstructural analysis. Therefore, addition of CNTs in YSZ coatings has a significant impact over the wear resistance and mechanical properties improvement of the coatings.

1. Introduction

Thermal barrier coatings (TBCs) are extensively used in aircraft engines, the power sector, nuclear reactors, and also in the automobile sector. The yttria-based ceramic coatings are widely recommended for improving the wear and corrosion resistance. In particular, yttria-stabilised zirconia (YSZ) coating is highly recommended as a thermal barrier coating for turbine engines to increase the wear resistance and also to protect the components from an aggressive oxidation environment. YSZ thermal barrier coatings (TBCs) deposited using atmospheric plasma spraying on nicked-based superalloy DZ125 substrate were examined by Wang et al. and found that the type of bonding, metallurgical structure, and YSZ coatings' porosity had improved [1]. The source of YSZ for the thermal spray process is in the form of micro-level and nano-level technology [2–4]. Initially, thermal barrier coatings are deposited using sputtering methods like physical vapour deposition (PVD), chemical vapour deposition (CVD), and electron beam assisted PVD process (EB-PVD) [5–7]. Later, these coatings are deposited with thermal spraying processes that are quite different from sputtering and molten deposition methods [8, 9]. However, it is reported that the ceramic coatings deposited using sputtering or thermal spraying processes are reflected with the presence of porosity in the microstructure of the coatings [10, 11].

It is important to note that the ceramic coatings are highly recommended for surface properties enhancement.

Especially, the ceramic coatings support to insulate the component from thermal ambient, increase the wear resistance, and also protect the surface from oxidation/corrosion resistance [12]. In addition to ceramic coatings, there are some hard metallic oxide/carbide coatings like tungsten carbide, titanium carbide, chromium oxide, and titanium oxide [13, 14]. The size of the powder material has also influenced in improving the metallurgical quality of the coatings [15]. The use of nickel-tungsten carbide (Ni-WC) powder in terms of nano structure will increase the strength in grain boundaries on deposition [16]. A step ahead, the coatings in the form ceramic and metallic carbide/oxide is used as a composite coating [17]. Influence of metallic carbide/oxide in the ceramic composite coating will subsequently increase the microhardness and wear resistance in the coatings [13]. In the view of coating powder deposit, the selection of appropriate coating process plays a vital role. The materials in the form of ceramic, metallic, carbide, and/or oxide in the form of composite coating depend on spray temperature. Plasma spray coating is one of the versatile processes to handle any form of coating material to deposit on the substrate surface. Metallurgical characteristics and mechanical properties of the coating are found better in atmospheric plasma-sprayed coatings [18].

In this research work, an attempt is made to study the tribological behaviour of plasma-sprayed YSZ coatings. To increase the strength and metallurgical bonding in the coatings, carbon nanotubes are used. It was found in earlier works that the carbon in carbon nanotubes (CNTs) forms a covalent bond with the parent material easily. On the other hand, the addition of carbon will also enrich the surface properties of the coatings in terms of increased surface hardness, good wear resistance, and controlled friction against the counter material [13].

In this present work, the CNTs in powder form are mixed with the ceramic feedstock powders of YSZ and then sprayed on the metallic substrates to obtain the corresponding coatings. The coatings are deposited using air plasma spraying (APS). However, it is believed that after adding the CNTs with ceramic feedstock, the pores are reduced in the coatings significantly with an astonishing bonding strength due to CNTs reinforcement.

2. Experimental Procedure

Yttria-stabilised zirconia (YSZ) feedstock powder was used for depositing the coatings on the mild steel substrate. To increase the bond strength and wear resistance, the carbon nanotubes (CNTs) were blended with the YSZ feedstock powder before spraying. The morphology of the CNTs mixed with YSZ powder and microstructure of coatings is observed under a high-resolution scanning electron microscope (SEM) at higher magnifications. CNT powder was procured from a standard supplier with a valid test report. The purity of the CNTs used was 98.9% with physical dimensions of ϕ 25 nm and 25 μm length with a bulk density of 0.14 g/cm^3. Ball mill (Make: SISCO) was used for the mechanical blending of CNTs with YSZ ceramic feedstock powder. The process conditions of ball milling are shown in Table 1.

Table 1: Process conditions for ball milling.

Parameter	Range	Units
Vail speed	400	rpm
Vial diameter	90	mm
Vial material	High chrome hard steel	—
Ball material	Tungsten ball	—
Milling type	Dry condition	—
Milling time	60	min

After ball milling, the thoroughly mixed composite powder was used for deposition of coatings using the air plasma spraying process. The air plasma spraying (APS) process is one of the best and versatile thermal spraying methods to deposit rare earth and ceramic materials also [9]. The process parameters used for the deposition of coatings are shown in Table 2. In this research work, the YSZ feedstock powder with three different weight percentage proportions of 1 wt.%, 3 wt.%, and 5 wt.% of CNTs reinforcement was used to deposit the coatings on the substrate material. A coating thickness of approximately 500 microns was maintained and evaluated through the cross-sectional micrographs.

The phases present in the powders and coatings were found using X-ray diffraction (XRD) analysis. The XRD studies were carried out using a PANalytical X'pertPRO (PW1070) X-ray diffractometer with CuKα radiation, operating at 40 kV voltage and 30 mA current, scanning step size of 0.0167°, and step time of 0.13 s. The microhardness measurements were carried out using an MMT_X7B microhardness tester (MAT Suzawa, Japan) with a Vickers indenter. The microhardness tests were conducted at a load of 100 g and a dwell time of 15 s at random locations on the cross-section of the coating and an average microhardness of 8–10 readings was computed. The wear performance of CNTs reinforced YSZ coatings was evaluated using a ball-on-disc tribometer following the ASTM G133-05 standards. The tungsten ball of 8 mm diameter was used as the counter body. The wear tests were performed considering three different parameters, namely: applied load (kgf), disc rotational speed (rpm), and test duration (min). The sliding distance of 300 m was kept constant. The wear test parameters are shown in Table 3. From the wear tests, the mass loss and wear rate are calculated. Subsequently, the morphology worn-out coating surfaces was also observed through a scanning electron microscope and the wear mechanism has been analyzed from micrographs.

3. Results and Discussion

The powder morphology of CNTs and YSZ powders is shown in Figures 1 and 2. The carbon nanotubes shown in Figure 1 were produced through a chemical vapour deposition process. CNT powder particles are spherical in shape with an average size of 25 microns.

The carbon nanotubes in different weight percentage proportions are added to the yttria-stabilised zirconia ceramic feedstock powder and the corresponding coatings are obtained using air plasma spraying. These CNTs reinforced

Table 2: Process parameters used for deposition of coatings using APS.

Parameter	Range	Units
Arc current	630	Amps
Arc voltage	55–75	Volts
Primary gas (argon)	43	lpm (litre per minute)
Secondary gas (hydrogen)	14	lpm (litre per minute)
Stand-off distance	100–125	mm
Powder feed rate	30	g/min

Table 3: Ball-on-disc wear test parameters.

Parameter	Range	Units
Applied load	0.5, 1.0, and 1.5	kgf
Disc rotating speed	319, 637, and 955	rpm
Test duration	10, 20, and 30	min
Sliding distance	300	m
Wear track diameter	10	mm

coatings were evaluated for phase analysis, microstructural characteristics, mechanical properties, and the wear characteristics. Figure 3 shows the optical microscopic image of YSZ mixed with CNTs at different percentage proportions. It is clear to infer from the optical microscopic image that the carbon nano particles have been dispersed throughout the coating. Microstructure also revealed the dark regions over a ceramic coating in a light colour. It has been postulated from the literature reports that the dark and white fringes are due to edges and boundaries during molten deposits [19].1% of CNT has been found to be scattered randomly in dark layers in YSZ and changes were revealed on the increase of weight percentage of CNT. Significantly 5% of CNT has been found uniformly dispersed in YSZ-based ceramic and justifiable in CNT dispersion. In addition, the percentage porosity of the thermally sprayed coatings is also studied with image analyser following the ASTM standard (of ASTM B 276) procedure. As reported in the literature, the addition of CNT will have surface reaction with the bonding material. In this case, the optical image reflects that the 5% of CNT has uniform distribution throughout the coating and 1% of CNT has less distribution. In contrast to the distribution, 1% of CNT has minimum porosity of 6.22% for a total observed area of 1.175 sq. mm. However, increase in CNT has maximum porosity of 16.53% and 16.78% for CNTs in 3% and 5% in weight proportion, respectively. The significance behind the increase in porosity in the YSZ coating is different from other processes. The use of MWCNT in YSZ ceramic material is highly reactive. In this way, the increase in CNT weight proportion is directly proportional to the porosity of the coating. During thermal spray process, the amount of heat generated will react with both YSZ and CNT to pay path to produce voids. However, the strength of the YSZ will be increased compared to the varying proportion of CNTs in the coating.

In order to confirm the presence of CNTs in the ceramic material, the X-ray diffractometric analysis is performed. For comparison, the XRD results of YSZ with different weight

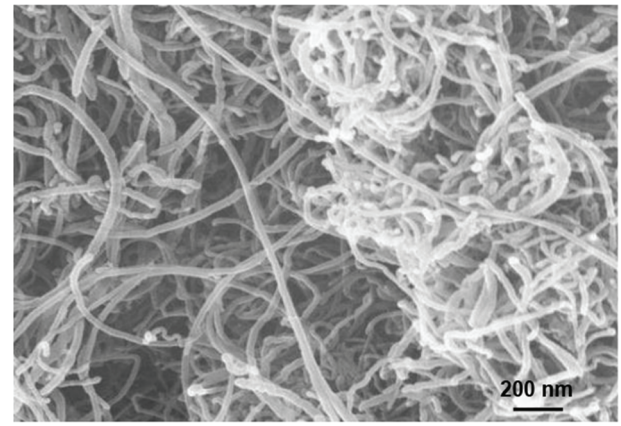

Figure 1: FE-SEM image of multiwalled carbon nano tubes.

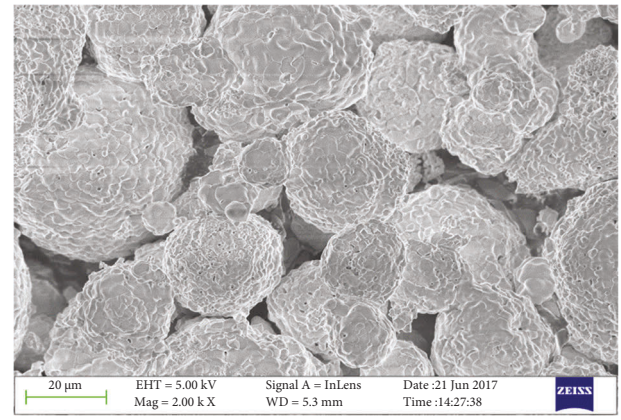

Figure 2: SEM image of yttria-stabilised zirconia powder used for thermal spray process.

proportion of CNT is assessed with pure YSZ material. The XRD report reflects the presence of zirconia in the form of monoclinic, tetragonal, and cubic phase. Different forms of zirconia in YSZ coatings indicate that yttria-stabilized zirconia is reactive at plasma spray temperature. At an angle of 30° (for 2θ representation), cubic phase has maximum intensity over a lattice (111). Subsequently, the XRD peaks for monoclinic structure is also reflected through the XRD analysis (see Figure 4). This reaction occurs as a result of yttria stabilisation and the formation of a complete solid solution during thermal spray deposition. In order to study the grain size and bonding strength of the particle deposited, the Scherrer equation is used and the average size of 25 nm is considered. For the YSZ with the CNT material, the presence of carbon is confirmed in the XRD peaks pattern. The intensity of carbon dispersion is clear to infer over the YSZ ceramic material. At the same time, the intensity of YSZ found was reduced while increasing the percentage of CNT weight percentage. Therefore, the presence of CNT in the YSZ thermal sprayed coating is confirmed through optical imaging and X-ray diffraction for further processing.

To discuss in detail about the coating thickness and metallurgical bonding, the thermally sprayed layer is polished following the standard procedure. Prepared samples are observed through an electron microscope to measure the

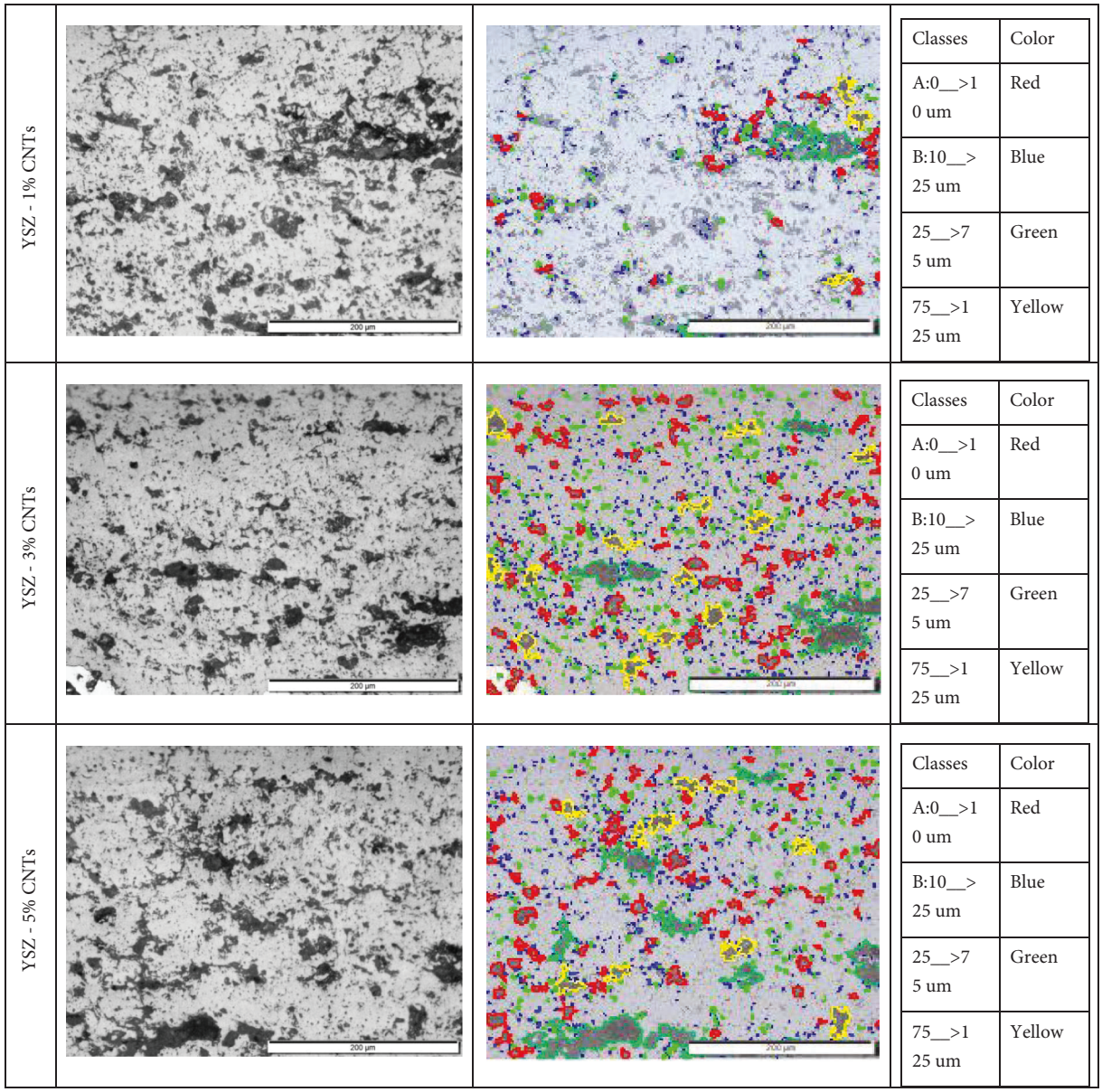

Figure 3: Optical image of YSZ with three different CNT proportion indicating the dispersion at higher magnification.

coating thickness and metallurgical bonding. Figure 5 shows the scanning electron microscopic images showing the bonding layer and coating thickness of YSZ reinforced with CNTs at different weight percentage proportions. The hatch geometry of the thermal spray layer is uniform throughout the splat deposit on the substrate material. Based on the SEM images, the achieved coating thickness was very close to the target thickness of 500 μm. Microscopic image also supports that the metallurgical bonding of the YSZ and CNTs coatings strongly adheres to the substrate material. In general, it is difficult to modify the surface of carbon steel as they are vulnerable to an aggressive environment. However, a successful deposition is noticed on mild steel substrates through the thermal spraying process in this work.

Microhardness of YSZ coating systems obtained with different percentage portions of the CNTs reinforcement is shown in Figure 6. Figure 6 shows that when the amount of CNTs in the coatings increases, the hardness of the coatings increases significantly. The percentage fluctuation of CNTs greatly affects the outcomes (i.e., 1, 3, and 5 wt.%). This is in accordance with the expectation that as the amount of CNTs in the coatings grows, porosity in the coatings reduces, hence hardness increases. Reference [20].

Further, thermally sprayed YSZ coatings obtained with different weight percentage proportions of CNTs addition are used to study the sliding wear behaviour of the coatings. The experimental investigation on sliding wear analysis is performed through a ball-on-disc tribometer. Schematic illustration of the ball-on-disc wear test process is shown in Figure 7. A 8 mm tungsten ball slides on a thermally sprayed YSZ-CNT coating at different speed at varying applied loaded condition. The experiments are conducted at

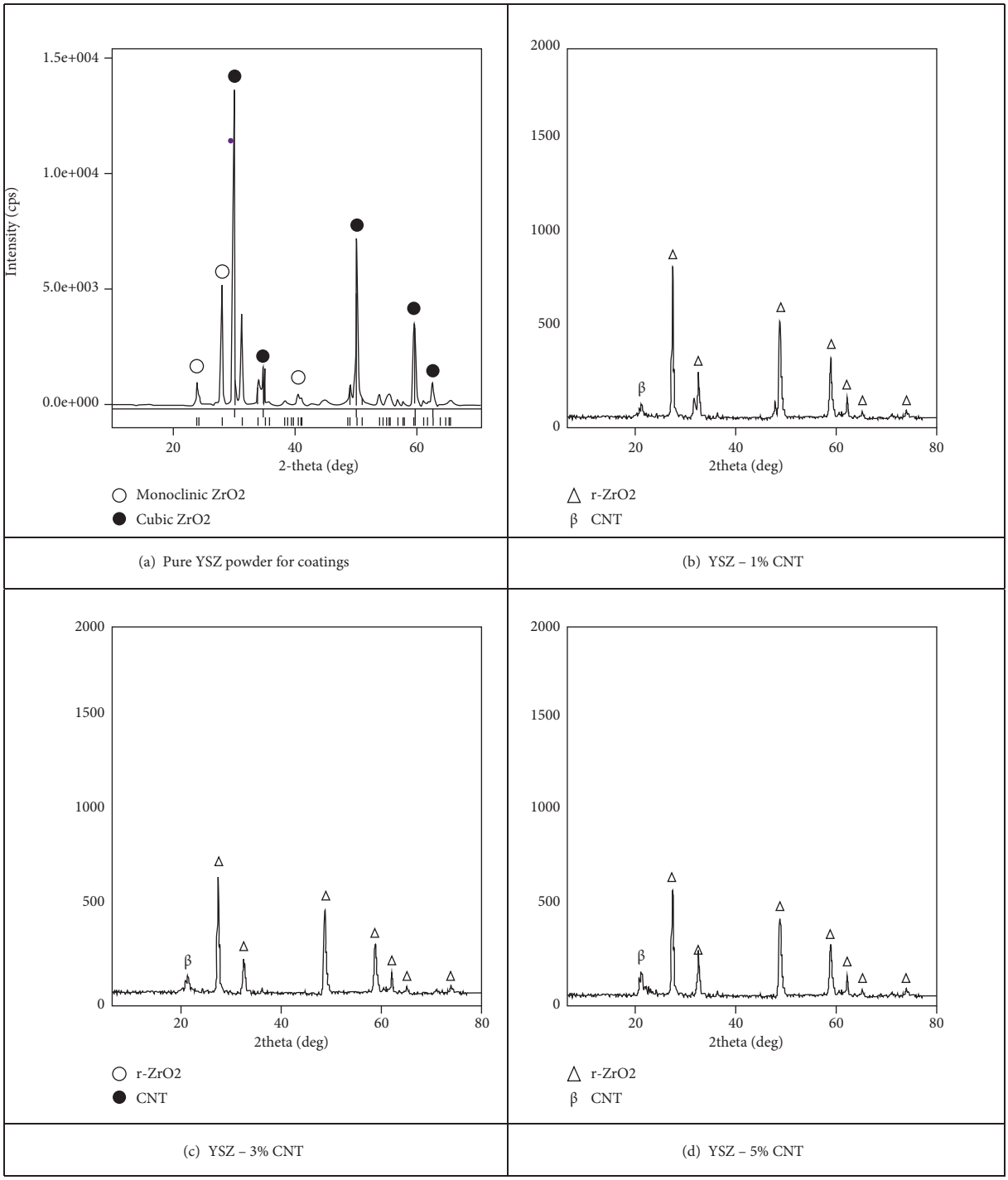

Figure 4: XRD peaks of (a) pure YSZ powder before spray and (b)–(d) after spray with CNT at different weight percentage proportions. (a) Pure YSZ powder for coatings. (b) YSZ-1% CNT. (c) YSZ-3% CNT. (d) YSZ-5% CNT.

different process conditions in nine different combinations by varying the applied load, disc rotating speed, sliding distance, and wear test time. At these test conditions, the experiments are conducted for individual material combination. Table 4 shows the combination of test conditions used for wear test.

From the wear analysis, the recorded responses on mass loss are given in the form of graphical representations as shown in Figure 8. It is clear to depict that the mass loss for 1% CNT in YSZ has a record of maximum value (0.0035 g) for an applied load 1.5 kgf rotating at 955 rpm. When the disc rotates at a maximum speed, the tangential force exerted will cross the tendency of threshold and friction force will be increased. To control the frictional force and its impact, it is proposed to minimise rotating speed and reduce applied load condition. However, for a specific condition, it is

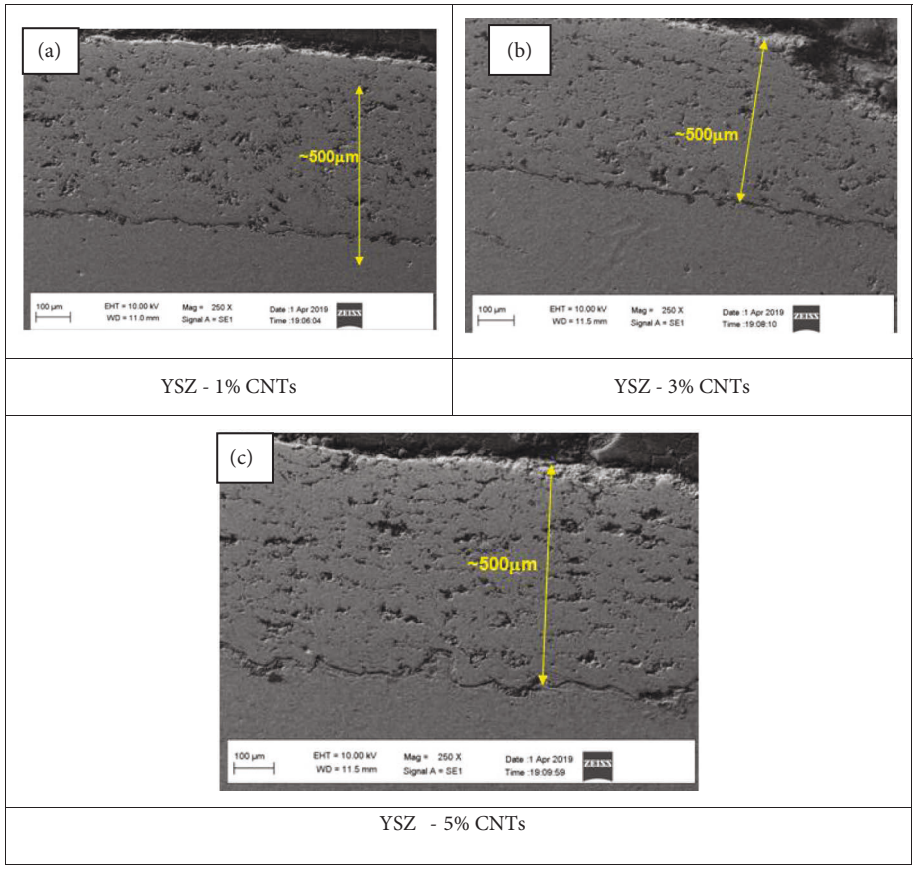

Figure 5: SEM image of YSZ coating with different percentage of CNT indicating the thickness of the coating. (a) YSZ-1% CNTs. (b) YSZ-3% CNTs. (c) YSZ-5% CNTs.

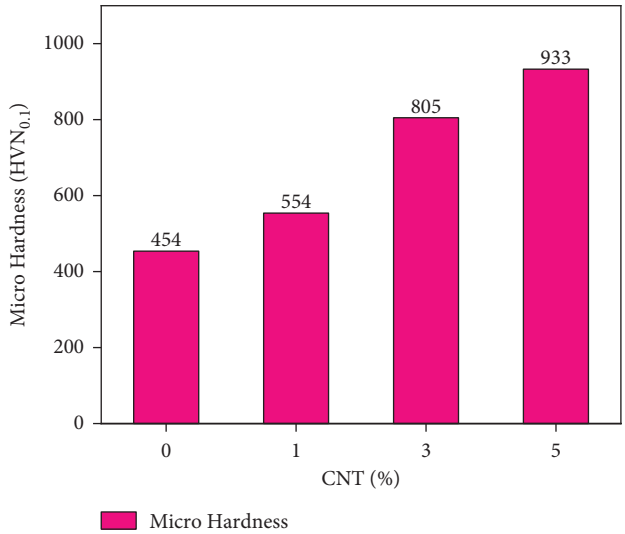

Figure 6: Microhardness of coating system at different percentage proportions of CNTs reinforcement.

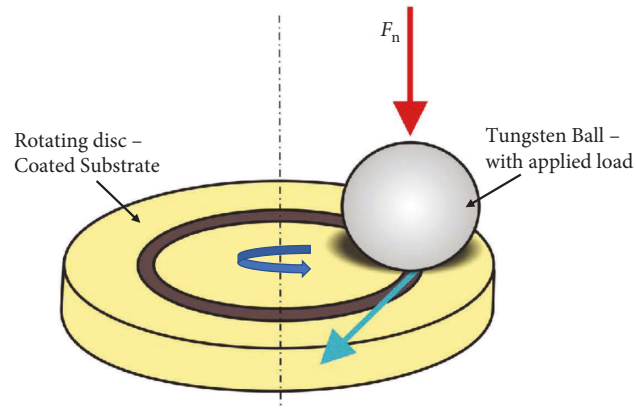

Figure 7: Schematic illustration of the ball-on-disc wear test process following the ASTM standard (ASTM G133-05) [21].

difficult to suggest these constraints (reducing speed and load) as they are designed for particular application. To meet out this situation, the addition of CNT in YSZ has produced good results in terms of mass loss. The mass loss for 3% CNT is 0.0032 g and for 5% CNT it is recorded as 0.003 g for the same process (955 rpm with 1.5 kgf) conditions. Subsequently, a very minimum loss (0.0017 g) is recorded for minimum speed (319 rpm) with applied load (0.5 kgf). It shows that the resistance of the YSZ has been increased with increase in CNT weight percentage.

The recorded response on wear resistance is given in the form of graphical representations as shown in Figure 9. The wear resistance is directly proportional to the hardness of the sliding surface. For a rotating ball, the hardness is 85 HRC

Table 4: Combination of test conditions used for wear test.

Test	Load (kgf)	Speed (rpm)	Distance (m)	Test duration (min)
1	1.5	955	300	10
2	1	955	300	10
3	0.5	955	300	10
4	1.5	637	300	15
5	1	637	300	15
6	0.5	637	300	15
7	1.5	319	300	30
8	1	319	300	30
9	0.5	319	300	30

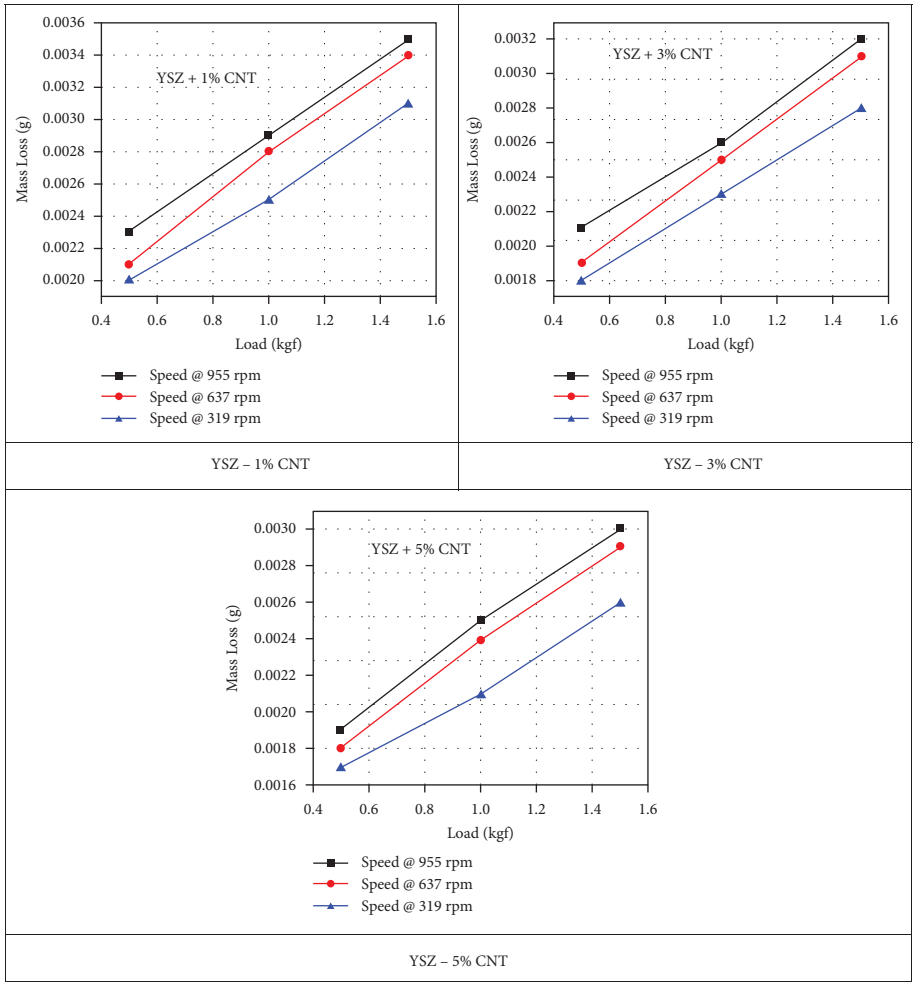

Figure 8: Mass loss measured during the experimentation with YSZ + CNT coating for different rotational speed.

and for the YSZ coating, it is 70 HRC [9]. Both the materials are rich in hardness compared to the substrate material. During sliding wear test, in addition to influence of surface hardness, the frictional energy generated will also highly influence to cause the wear. It is observed that the reinforcement of CNT in the YSZ has simultaneously increased the surface hardness of the coating. Behaviour of CNT in YSZ reveals the performance like a diamond during sliding wear analysis. The maximum wear resistance of 3980 Nm/mm^2 is recorded for 5% of CNT in YSZ. Wear resistance is also influenced by the process conditions such as applied load and sliding velocity or speed. Further, the worn surfaces of coatings are evaluated through electron microscope to study the wear mechanism and surface topography.

Worn surface of YSZ-CNT coating observed through electron microscopy is shown in Figure 10. For all the conditions, the wear tracks are clear to highlight the direction of the roller (hard tungsten ball) over YSZ-CNT coatings. Degrees of freedom for the rolling ball is free to all the directions and it has induced the surface on coatings with

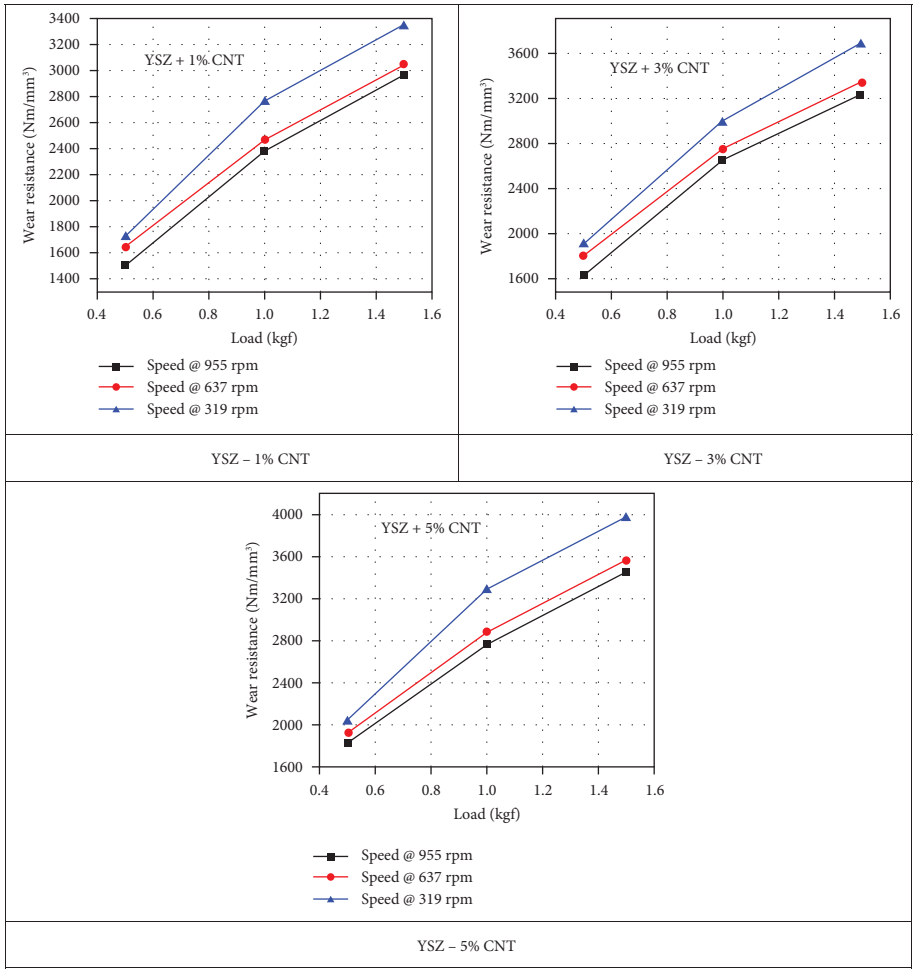

Figure 9: Calculated wear resistance for the test experiments on YSZ + CNT coatings for different rotational speed.

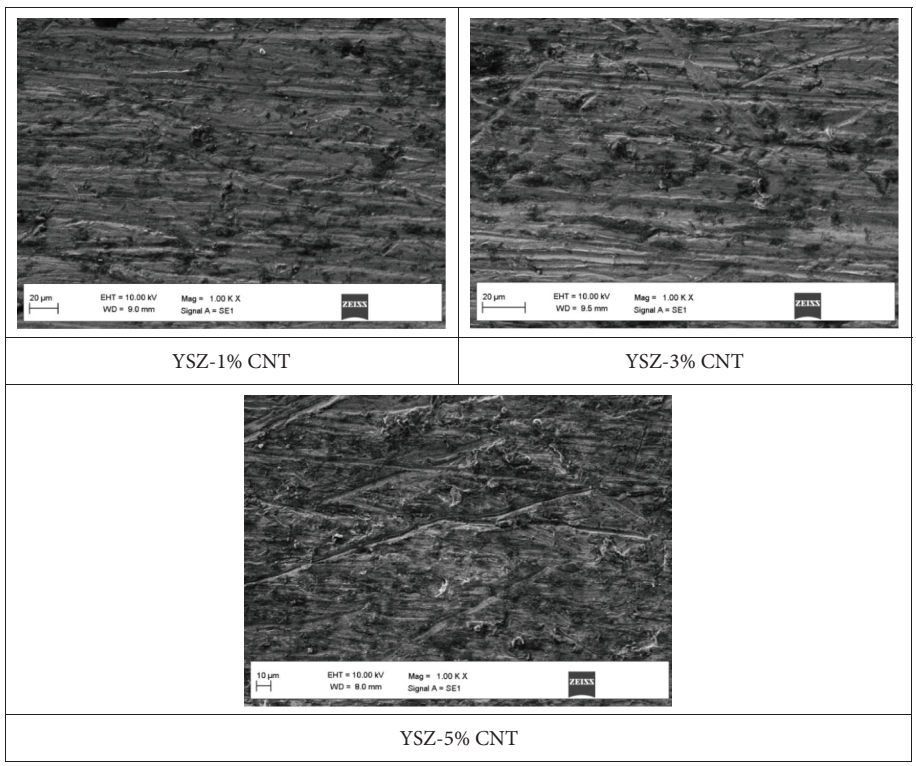

Figure 10: Surface topography of worn surface with different combination of CNT in YSZ coating.

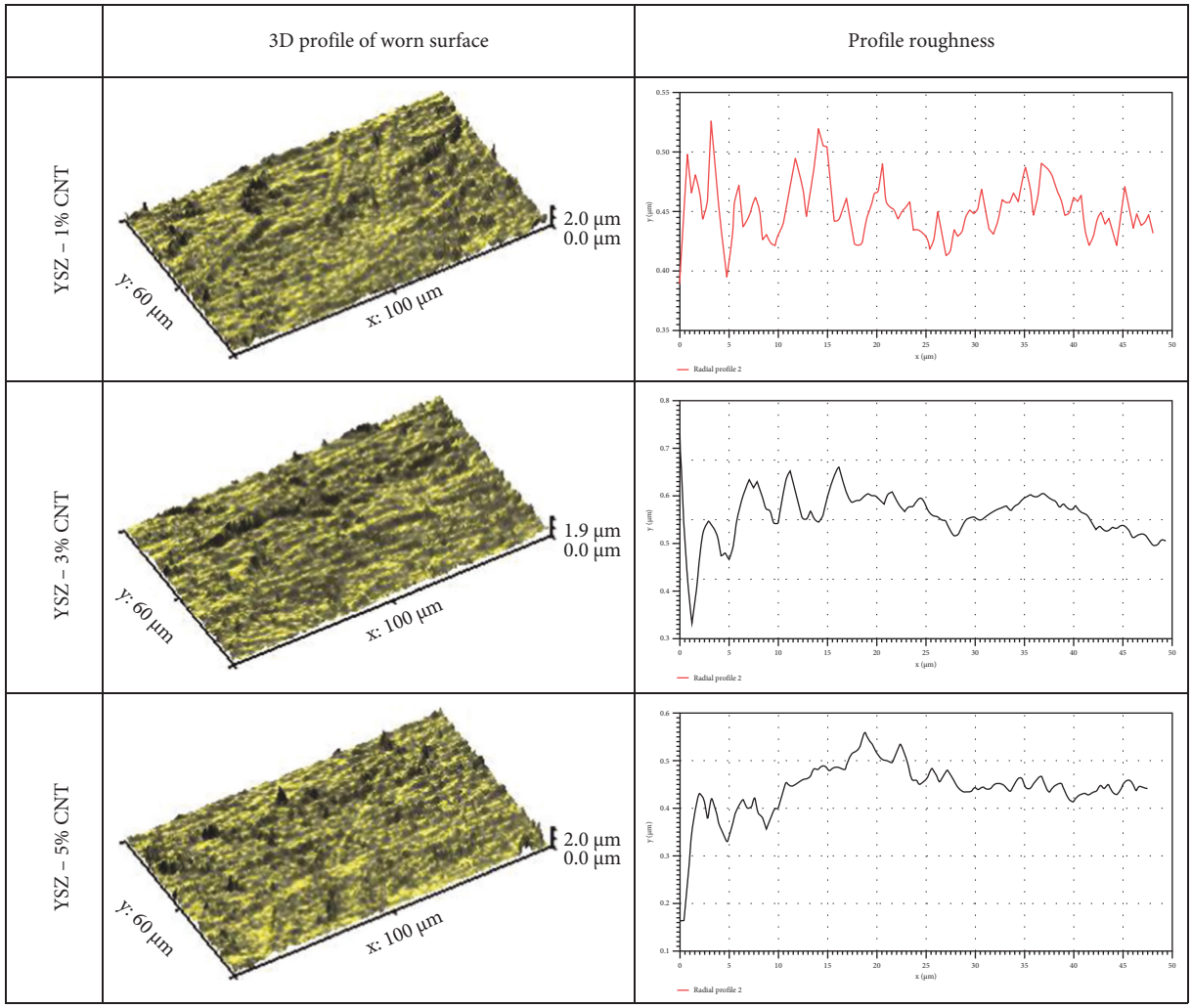

Figure 11: 3D profile of worn surface on YSZ-CNT coatings.

point. The point of impress (of hard ball) over the coating is less (approximately 30 microns) and the total load applied on the ball will cause severity in surface damage. Moreover, the ceramic materials are vulnerable (severity in cracks/fracture) towards the point load with tangential (frictional) force. In this work, the metallurgical bonding of the YSZ ceramic material and addition of CNT and simultaneously the properties of the coating have been increased to resist the friction of the rolling ball. The mechanism involved in this research confirms that there is no adhesion or erosion of hard particle over the worn surface. It has induced the coating to make a score mark (mild abrasion) in the form of continuous tracks. To discuss in detail, the worn surface is analyzed using a 3D profile metre. Figure 11 shows the 3D profile and its surface area roughness of the worn surface on YSZ-CNT coatings after wear analysis. The average surface roughness of the worn area is 40–55 μm and it is measured for exposed surface area. Maximum surface roughness is for 5% of CNT, which is around 52–55 μm. When the hard ball slides on the coated surface, the voids/pores are compressed, and the surface protrudes with maximum peaks and valleies. This is not a negative sign of result, and it is due to compressive strength over pores on ceramic coatings. Therefore, the presence of CNT in YSZ has subsequently increased the wear resistance and protected the substrate from maximum wear in terms of material loss and increased the coating life.

4. Conclusions

Experimental investigation on plasma-sprayed yttria-stabilised zirconia coatings reinforced with carbon nano tubes has been performed to study the mechanical properties and wear characteristics. The following are the conclusions with technical justifications to recommend the CNT-YSZ thermal spray coatings.

The addition of CNTs in the ceramic coatings has increased the porosity of the coating. This is due to the metallurgical fusion and surface reaction of CNTs with YSZ. As a result, the metallurgical reaction between the elements has simultaneously increased the surface hardness. The presence of CNTs in YSZ has maximum surface hardness of 566.72 Hv, 507.35 Hv for 3% CNT, and 493.19 Hv for 1% CNT. Compared to the hardness of pure APS-sprayed YSZ

(440.81 Hv), an increase in hardness was noticed with an increase in CNT. The metallurgical bonding was found to be strong with the substrate material and the thickness of the coating was uniform throughout the section. The dark in colour indicates the surface reaction of CNT with ceramic material. Mass loss of 1% CNT in YSZ found maximum of 0.0035 g and minimum of 0.0017 g for 5% CNT in YSZ plasma coated layer. Pure ceramics are possible to abrade and pull out of particles. However, the addition of CNT has increased the bonding strength and surface hardness to resist the sliding wear. Subsequently, the surface was found with minimum wear and less wear scars on 5% CNT. Therefore, the presence of YSZ with CNT has substantially increased the surface hardness and the wear resistance has been increased.

Data Availability

All data generated or analyzed during this study are included in this published article.

Ethical Approval

The paper is not submitted to any other journal. The authors declare that they have no known competing financial interest or personal relationships that could have appeared to influence the work reported in this paper.

Consent

All authors agreed to participate in this research study and gave permission to publish the study.

Disclosure

The authors declare that they have no conflicts of interest or personal relationships that could have appeared to influence the work reported in this paper.

Conflicts of Interest

The authors declare that they have no conflicts of interest.

Authors' Contributions

All authors contributed to the study conception and design. Material preparation, data collection, and analysis were performed by K. Chaithanya, and B. Venkateshwarlu. The first draft of the manuscript was written by K. Chaithanya and all authors commented on previous versions of the manuscript. All authors read and approved the final manuscript.

References

[1] Y. Wang, M. X. Li, and H. L. Suo, "Mechanical properties of YSZ thermal barrier coatings with segmented structure," *Surface Engineering*, vol. 28, no. 5, pp. 329–332, 2012.

[2] Y. Bai, Y. H. Wang, Z. Wang, Q. Q. Fu, and Z. H. Han, "Influence of unmelted nanoparticles on properties of YSZ nano-coatings," *Surface Engineering*, vol. 30, no. 8, pp. 568–572, 2014.

[3] D. Ghosh, S. Das, H. Roy, and S. K. Mitra, "Oxidation behaviour of nanostructured YSZ plasma sprayed coated Inconel alloy," *Surface Engineering*, vol. 34, no. 1, pp. 22–29, 2018.

[4] R. Liu and L. Shi, "Formation of t'-YSZ nanocoating from composite sols," *Surface Engineering*, vol. 29, no. 9, pp. 700–702, 2013.

[5] Q.-Y. Chen, C.-X. Li, J.-Z. Zhao, G.-J. Yang, and C.-J. Li, "Microstructure of YSZ coatings deposited by PS-PVD using 45 kW shrouded plasma torch," *Materials and Manufacturing Processes*, vol. 31, no. 9, pp. 1183–1191, 2016.

[6] J. V. Garcia and T. Goto, "Thermal barrier coatings produced by chemical vapor deposition," *Science and Technology of Advanced Materials*, vol. 4, pp. 397–402, 2003.

[7] M. Góral, R. Swadźba, and T. Kubaszek, "TEM investigations of TGO formation during cyclic oxidation in two- and three-layered Thermal Barrier Coatings produced using LPPS, CVD and PS-PVD methods," *Surface and Coatings Technology*, vol. 394, Article ID 125875, 2020.

[8] M. Adam Khan, S. Sundarrajan, and S. Natarajan, "Design and statistical analysis of plasma coatings on superalloy for gas turbine applications," *Materials at High Temperatures*, vol. 34, no. 1, pp. 12–21, 2016.

[9] A. K. M. Basha, S. Srinivasan, and N. Srinivasan, "Studies on thermally grown oxide as an interface between plasma-sprayed coatings and a nickel-based superalloy substrate," *International Journal of Minerals, Metallurgy and Materials*, vol. 24, no. 6, pp. 681–690, 2017.

[10] T. Nakamura, G. Qian, and C. C. Berndt, "Effects of pores on mechanical properties of plasma-sprayed ceramic coatings," *Journal of the American Ceramic Society*, vol. 83, no. 3, pp. 578–584, 2004.

[11] X. Li, X. Yin, L. Zhang, and T. Pan, "Comparison in microstructure and mechanical properties of porous Si3N4 ceramics with SiC and Si3N4 coatings," *Materials Science and Engineering: A*, vol. 527, no. 1-2, pp. 103–109, 2009.

[12] S. Maharajan, D. Ravindran, S. Rajakarunakaran, and M. Adam Khan, "Analysis of surface properties of tungsten carbide (WC) coating over austenitic stainless steel (SS316) using plasma spray process," *Materials Today Proceedings*, vol. 27, pp. 2463–2468, 2020.

[13] Q. Y. Hou, L. M. Luo, Z. Y. Huang, P. Wang, T. T. Ding, and Y. C. Wu, "Comparison of W-TiC composite coatings fabricated by atmospheric plasma spraying and supersonic atmospheric plasma spraying," *Fusion Engineering and Design*, vol. 105, pp. 77–85, 2016.

[14] M. J. Ghazali, S. M. Forghani, N. Hassanuddin, A. Muchtar, and A. R. Daud, "Comparative wear study of plasma sprayed TiO2 and Al2O3–TiO2 on mild steels," *Tribology International*, vol. 93, pp. 681–686, 2016.

[15] R. J. K. Wood, S. Herd, and M. R. Thakare, "A critical review of the tribocorrosion of cemented and thermal sprayed tungsten carbide," *Tribology International*, vol. 119, pp. 491–509, 2018.

[16] M. Sabzi, S. M. Dezfuli, and S. M. Far, "Deposition of Nitungsten carbide nano composite coating by TIG welding: characterization and control of microstructure and wear/corrosion responses," *Ceramics International*, vol. 44, no. 18, pp. 22816–22829, 2018.

[17] S. Khandanjou, M. Ghoranneviss, and S. Saviz, "The detailed analysis of the spray time effects of the aluminium coating using self-generated atmospheric plasma spray system on the

microstructure and corrosion behaviour," *Results in Physics*, vol. 7, pp. 1440–1445, 2017.

[18] M. A. Khan, S. Sundarrajan, M. Duraiselvam, S. Natarajan, and A. S. Kumar, "Sliding wear behaviour of plasma sprayed coatings on nickel based superalloy," *Surface Engineering*, vol. 33, no. 1, pp. 35–41, 2017.

[19] U. Klement, J. Ekberg, S. Creci, and S. T. Kelly, "Porosity measurements in suspension plasma sprayed YSZ coatings using NMR cryoporometry and X-ray microscopy," *Journal of Coatings Technology and Research*, vol. 15, no. 4, pp. 753–757, 2018.

[20] S. Bilgin, O. Güler, Ü. Alver, F. Erdemir, M. Aslan, and A. Çanakçı, "Effect of TiN, TiAlCN, AlCrN, and AlTiN ceramic coatings on corrosion behavior of tungsten carbide tool," *Journal of the Australian Ceramic Society*, vol. 57, no. 1, pp. 263–273, 2021.

[21] Astm G133-05, *Standard Test Method for Linearly Reciprocating Ball-on-Flat Sliding Wear*, Standards & Publications, Ohio, OH, USA, 2016.